Supplementary Information

Predicting Sizes of Hexagonal and Gyroid Metal Nanostructures from Liquid Crystal Templating

Kaleem A. Asghar, Daniel Rowlands, Joanne M. Elliott and Adam M. Squires

Supplementary Information

A) Derivation of structural relations

A_n is estimated from the lattice parameter a of a fluid lamellar phase of surfactant volume fraction ϕ_{surf} by assuming that the bilayer thickness is twice the length of the molecule, and that the cross-sectional area of the molecule takes a constant value A_n. The volume fraction of surfactant is therefore equal to $\phi_{surf} = \frac{2v}{A_n a}$ and from this we obtain

$$A_n = \frac{2v}{a\,\phi_{surf}} \qquad \text{Equation S1}$$

In order to determine v_n, in other words, to locate the position of the area neutral surface within the molecule, we use data from the hexagonal phase. We assume that the hexagonal phase consists of surfactant cylinders whose radius r defines the distance from the centre of the cylinder to the surfactant-water interface. This is shown in Figure SI1. We assume that changing the water volume fraction of the liquid crystalline mixture changes the separation of these cylinders, but keeps their radius constant.

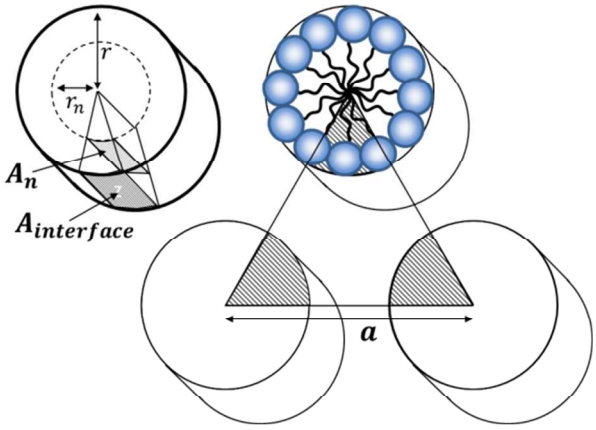

SI1: Schematic showing location of surfactant-water interface and area neutral surface in a hexagonal (H_1) phase. Lattice parameter = a; area per molecule at area neutral surface and surfactant-water interface = A_n , $A_{interface}$ respectively; radius of area neutral surface and surfactant-water interface = r_n, r respectively.

If we consider a triangle formed from the centres of adjacent surfactant cylinders, the length of side of this triangle is the lattice parameter a, and its area is $\frac{\sqrt{3}a^2}{4}$. Of this, the area that lies within the surfactant cylinders (shown as shaded regions in Figure SI1) is $\frac{\pi r^2}{2}$. The fraction of the area of the triangle that this shaded region represents is equal to the volume fraction of surfactant; thus, $\phi_{surf} = \frac{2\pi\, r^2}{\sqrt{3}a^2}$. Rearranging this gives the radius of the surfactant cylinders

$$r = \sqrt{\frac{\sqrt{3}a^2\phi_{surf}}{2\,\pi}} \qquad \text{Equation S2}$$

At the surfactant-water interface, the area per molecule, $A_{interface}$, is greater than A_n, the value at the area neutral surface. The ratio of the cross-sectional area of the interface cylinder to its circumference is equal to the ratio of v to $A_{interface}$:

$\frac{v}{A_{interface}} = \frac{\pi r^2}{2\pi r} = \frac{r}{2}$ from which we obtain

$A_{interface} = \frac{2v}{r}$ Equation S3

which we can estimate using values of v and r from Equations S1 and S2 respectively.

The area neutral surface is a concentric cylinder lying within the surfactant region, with a smaller radius, r_n (Figure SI1). Similar considerations give

$A_n = \frac{2v_n}{r_n}$ Equation S4

Since $\left(\frac{r_n}{r}\right) = \left(\frac{A_n}{A_{interface}}\right)$ (Figure SI1), we can combine Equations S3 and S4 to give

$v_n = v\left(\frac{A_n}{A_{interface}}\right)^2$ Equation S5

Once the molecular parameters v, v_n and A_n are all known for a particular surfactant, the relationship between lattice parameter and surfactant volume fraction for any lamellar, hexagonal or gyroid bicontinuous cubic phase may be calculated as follows:

For the lamellar phase, we rearrange equation S1 to give

$\phi_{surf} = \frac{2v}{a\,A_n}$ Equation S6

For the hexagonal phase, we combine equations S2, S3 and S5 to give

$\phi_{surf} = \frac{8\pi}{\sqrt{3}}\frac{v_n v}{(A_n a)^2}$ Equation S7

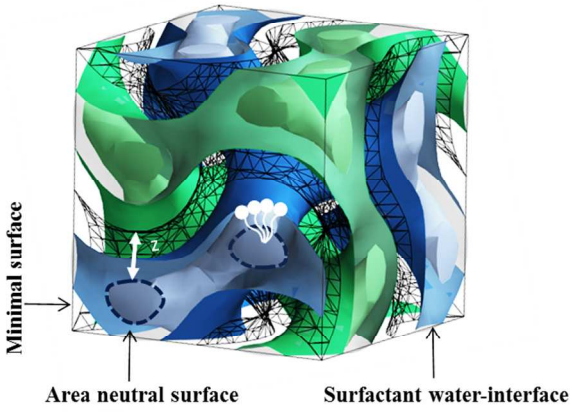

SI2: A schematic diagram of a double gyroid bicontinuous cubic phase V_I.

For the gyroid cubic phase, we assume that the area neutral surfaces lie parallel to the triply periodic minimal surface that passes through the middle of the water region (as do the surfactant-water interfaces). We consider the two area neutral surfaces to lie a distance z away from the minimal surface, on either side. This is illustrated in Figure SI2. In one particular bicontinuous cubic phase, z remains constant over

the surface. However, for different samples with different surfactant volume fractions and different lattice parameters, we allow z to change; the molecular parameters v, v_n and A_n remain constant.

An analogous system exists in the inverse bicontinuous cubic phases, where the minimal surface passes through the centre of a surfactant bilayer; similar analysis has been carried out on these structures, again employing a parallel interface model similar to the one we adopt here.[1]

The average value for the Gaussian curvature of the minimal surface is given by

$$< K > = \frac{2\pi\chi}{\sigma_0 a^2}$$

Where χ and σ_0 are the Euler characteristic and the dimensionless area per unit cell, taking values of -8 and 3.091 respectively for the gyroid minimal surface.[2]

In general, if we consider a patch of a surface projected a distance z away from a patch of minimal surface of area A(0), the area of the patch of parallel surface, A(z), and the volume between it and the minimal surface[2], v(z), are given by

$$A(z) = A(0)(1 + Kz^2) \qquad \text{and} \qquad v(z) = A(0)z\left(1 + \frac{1}{3}K\,z^2\right)$$

In a unit cell of normal topology bicontinuous cubic phase, there are two such surfaces, which are the area neutral surfaces for each surfactant network. The area of the minimal surface in the unit cell is $A(0) = \sigma_0 a^2$, and so the total area of area neutral surface in one unit cell is given by

$$A(z) = 2\,\sigma_0\,a^2\left(1 + \frac{2\pi\chi}{\sigma_0 a^2}\,z^2\right) = n_{cell} A_n \qquad \text{Equation S8}$$

where n_{cell} is the number of surfactant molecules in the unit cell.

The region lying between the minimal surface and two area neutral surfaces contains the water, and the surfactant headgroups. The remaining volume, on the tail side of the area neutral surface is given by

$$a^3 - 2\,\sigma_0\,a^2\,z\left(1 + \frac{2\pi\chi}{3\sigma_0 a^2}\,z^2\right) = n_{cell}\,v_n \qquad \text{Equation S9}$$

Equating n_{cell} from equations S8 and S9 gives

$$n_{cell} = \frac{2\,\sigma_0 a^2}{A_n}\left(1 + \frac{2\pi\chi}{\sigma_0 a^2}\,z^2\right) = \frac{\left(a^3 - 2\,\sigma_0\,a^2\,z\left(1 + \frac{2\pi\chi}{3\sigma_0 a^2}\,z^2\right)\right)}{v_n}$$

Equation S10

This can be solved to determine z and n_{cell} for each lattice parameter. The volume fraction of surfactant is then determined for this lattice parameter using

$$\phi_{surf} = \frac{n_{cell} v}{a^3}$$

B) Experimental data for lattice parameter as function of temperature

To investigate the effect of temperatures on lattice parameter (a) values of different mixtures of Brij 56/H_2O exhibiting hexagonal, gyroid and lamellar phases, temperature controlled SAXS experiments were carried out. Figure SI shows lattice parameter variations as a function of temperature for 40 and 68 wt% of Brij 56/H_2O. All results show that the lattice parameters of the different phases of both the surfactants are approximately independent of temperature, however any noticeable change in the lattice parameter plots is possibly because of the dehydration of the head groups of the surfactants. [3]

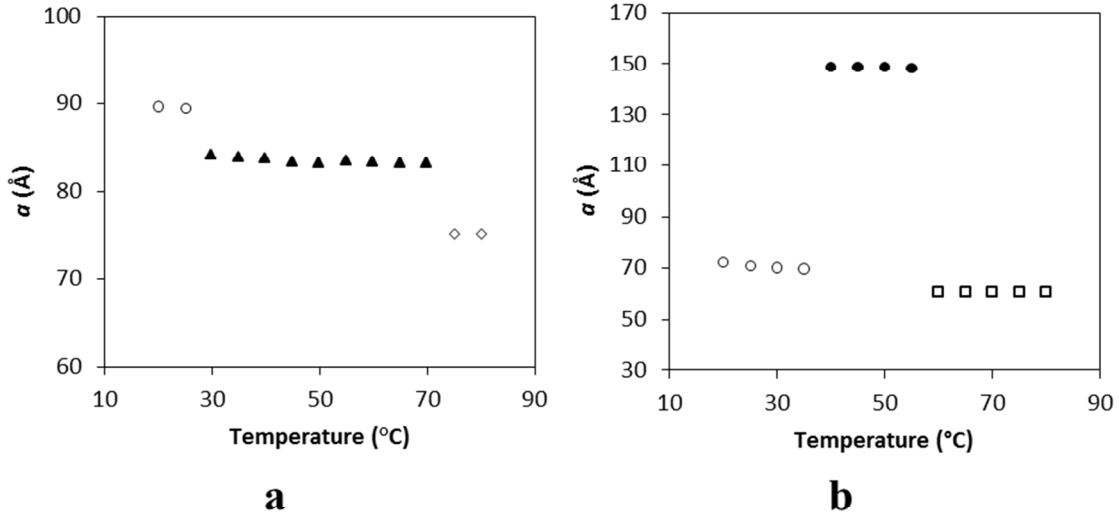

SI3: A Lattice parameter variations as a function of temperature for binary mixtures of (a) 40 wt% Brij 56/H_2O and (b) 68 wt% Brij 56/H_2O showing crystalline (empty circles), hexagonal (solid triangles), gyroid (solid circles), lamellar (empty squares) and micellar (empty diamonds) phases at different temperatures.

C) Compositions of mixtures used

Table SI1(a). Binary mixtures of Brij 56/H_2O with different wt% compositions and volume fractions (ϕ) used to prepare hexagonal (H_I) phases.

wt% Brij 56	35	40	45	50	55	60	65
wt% H_2O	65	60	55	50	45	40	35
ϕ_{Brij56}	0.3553	0.4055	0.4557	0.5058	0.5557	0.6055	0.6552
ϕ_{H_2O}	0.6446	0.5944	0.5442	0.4941	0.4442	0.3944	0.3447

Table SI1(b). Pseudo ternary mixtures of Brij 56/hexadecane/H_2O with different wt% compositions and volume fractions (ϕ) used to prepare hexagonal (H_I) phases.

wt% Brij 56	55	50	47.5
wt% hexadecane	0	5	7.5
wt% H_2O	45	45	45
ϕ_{Brij56}	0.5557	0.4985	0.4705
$\phi_{\text{hexadecane}}$	0	0.0630	0.0939
ϕ_{H_2O}	0.4442	0.4384	0.4355

Table SI1(c). Binary mixtures of Brij 56/H_2O with different wt% compositions and volume fractions (ϕ) used for gyroid (V_I) phases.

Mixtures	a	b	c	d	e	f	g	h	i	j
wt% Brij 56	60	61	62	63	64	65	66	67	68	69
wt% H_2O	40	39	38	37	36	35	34	33	32	31
ϕ_{Brij56}	0.6055	0.6155	0.6254	0.6354	0.6453	0.6552	0.6652	0.6751	0.6850	0.6949
ϕ_{H_2O}	0.3944	0.3844	0.3745	0.3645	0.3546	0.3447	0.3347	0.3248	0.3149	0.3050
T (°C)	55	55	50	50	50	50	45	45	45	45

Table SI1(d). Binary mixtures of Brij 56/H_2O with different wt% compositions and volume fractions (ϕ) used for lamellar (L_α) phases.

wt% Brij 56	68	75	80
wt% H_2O	32	25	20
ϕ_{Brij56}	0.6850	0.7543	0.8036
ϕ_{H_2O}	0.3149	0.2456	0.1963
T (°C)	50	45	45

Mixtures used to prepare mesoporous platinum films

Table SI1(e). Pseudo binary mixtures of Brij 56/HCPA with different wt% compositions and volume fractions (ϕ) for the preparation of hexagonal (H_I) phases.

wt% Brij 56	40	50	60
wt% HCPA	60	50	40
ϕ_{Brij56}	0.4174	0.5180	0.6171
ϕ_{HCPA}	0.5825	0.4819	0.3828

Table SI1(f). Pseudo ternary mixtures of Brij 56/hexadecane/HCPA with different wt% compositions and volume fractions (ϕ) used for hexagonal (H_I) phases.

wt% Brij 56	55	50	47.5
wt% hexadecane	0	5	7.5
wt% HCPA	45	45	45
ϕ_{Brij56}	0.5677	0.5092	0.4805
$\phi_{\text{hexadecane}}$	0	0.0643	0.0958
ϕ_{HCPA}	0.4322	0.4264	0.4235

Table SI1(g). Binary mixtures of Brij 56/HCPA with different wt% compositions and volume fractions (ϕ) for gyroid (V_I) phases.

Mixtures	a	b
wt% Brij 56	60	68
wt% HCPA	40	32
ϕ_{Brij56}	0.6171	0.6954
ϕ_{HCPA}	0.3828	0.3045
T (°C)	55	40

D) TEM images

The structure and the mesoporosity of electrochemically deposited (H_1-ePt) and (V_1-ePt) films prepared from the H_1 and V_1 templating mixtures were also analysed by transmission electron microscopy. Figure SI5(a-c) shows transmission electron micrographs for mesoporous (H_1-ePt) films with pores approximately side-on, templated from different ternary hexadecane / Brij 56 / HCPA mixtures on increasing hexadecane content. Figure SI5(d) shows a mesoporous (V_1-ePt) film. Figure SI5 (e-j) shows mesoporous H_1-ePt with approximately end-on pores; (e)-(g) were templated from binary mixtures on increasing Brij-56 content, and (h)-(j) from ternary mixtures on increasing hexadecane content.

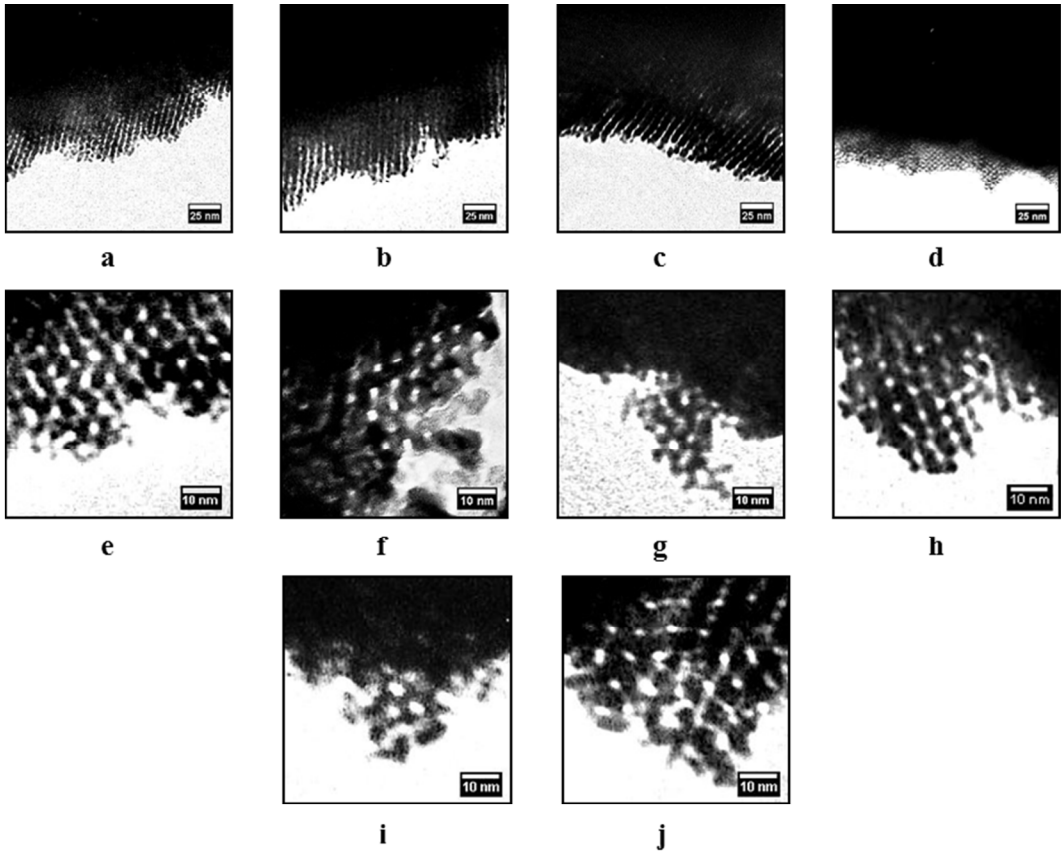

Figure SI4. Transmission electron microscopy images of H_1-ePt) and V_1-ePt films. (a-c) H_1-ePt films templated from mixtures of composition ($\phi_{hexadecane}$:ϕ_{Brij56}:ϕ_{HCPA}) = (0:0.57:43), (0.065:0.50:0.43) and (0.10:0.46: 0.43) respectively; (d) V_1-ePt film templated from (ϕ_{Brij56}:ϕ_{HCPA}) = (0.70:0.30). (e-g) H_1-ePt films templated from (ϕ_{Brij56}:ϕ_{HCPA}) = (0.42:0.58), (0.52:0.48) and (0.62:0.38) respectively. (h-j) H_1-ePt films templated from ($\phi_{hexadecane}$:ϕ_{Brij56}:ϕ_{HCPA}) = (0:0.57:43), (0.065:0.50:0.43) and (0.10:0.46: 0.43) respectively

The lattice parameters determined from the TEM images do not exactly agree with those from SAXS, showing typically about 4-7 % discrepancy. We consider SAXS determination to be more reliable for a number of reasons. First, the TEM images only shows a very small portion of the sample, while during SAXS analysis the sample is averaged macroscopically over an area the size of the X-ray beam, approx. 400 x 800 μm. Furthermore, we selectively image only those sections of the sample that are sufficiently thin to allow transmission of electrons. These sections are more likely to have undergone distortion on removal from the electrode surface; indeed, in the images shown, the actual pore sizes vary, especially towards the edge of the metal. Finally, in general the determination of lattice parameter in hexagonally arranged templated materials using TEM strongly depend on the orientation and the alignment of specimen observed under the microscope. S. Nakahara et al,[4,5] have nicely explained the problems associated with lattice parameter determination in analogous hexagonally arranged mesoporous silica materials. Therefore, while the measured dimensions show qualitative relative trends, we do not consider them to be quantitatively reliable.

E) Further Fitting

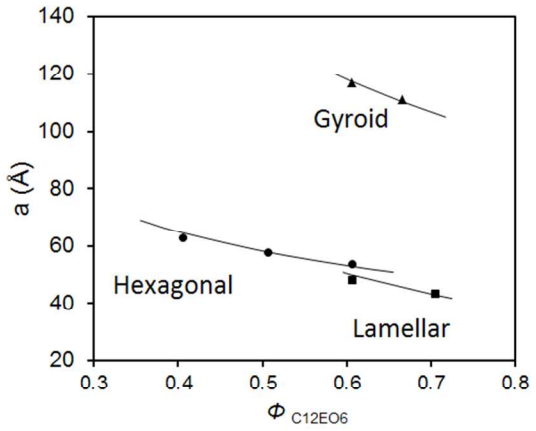

Figure SI5: lattice parameter vs surfactant volume fraction data for phases formed by binary mixtures of water and the surfactant C12EO6 (molecular formula $C_{12}H_{25}[OCH_2CH_2]_6OH$). All data were obtained at 20 °C apart from the lower surfactant content lamellar phase data point, which was obtained at 35 °C. Lines were obtained using the theoretical approach described in the paper with v =765 Å^3, A_n =50 Å^2 and v_n =390 Å^3.

References:

(1) Templer, R. H.; Seddon, J. M.; Warrender, N. A.; Syrykh, A.; Huang, Z.; Winter, R.; Erbes, J. *J. Phys. Chem. B* **1998**, *102*, 7251.

(2) Templer, R. H. *Langmuir* **1995**, *11*, 334.

(3) Amar-Yuli, I.; Aserin, A.; Garti, N. *J. Phys. Chem. B* **2008**, *112*, 10171.

(4) Hudson, S.; Tanner, D. A.; Redington, W.; Magner, E.; Hodnett, K.; Nakahara, S. *Phys. Chem. Chem. Phys.* **2006**, *8*, 3467.

(5) Nakahara, S.; Tanner, D. A.; Hudson, S.; Magner, E.; Redington, W.; Hodnett, K. *Phys. Chem. Chem. Phys.* **2011**, *13*, 1189.